

## Electrical characteristics and efficiency of single-layer organic light-emitting diodes

G. G. Malliaras,\* J. R. Salem, P. J. Brock, and C. Scott

IBM Research Division, Almaden Research Center, 650 Harry Road, San Jose, California 95120

(Received 24 August 1998)

We have measured the electrical characteristics and the efficiencies of single-layer organic light-emitting diodes based on poly[2-methoxy-5-(2-ethylhexoxy)-1,4-phenylene vinylene] (MEH-PPV), with Au anodes and Ca, Al, and Au cathodes. We show that proper accounting of the built-in potential leads to a consistent description of the current-voltage data. For the case of Au and Al cathodes, the current under forward bias is dominated by holes injected from the anode and is space-charge limited with a field-dependent hole mobility. The Ca cathode is capable of injecting a space-charge-limited electron current. [S0163-1829(98)52844-5]

Organic light-emitting diodes (OLED's) have emerged over the past ten years as viable candidates for application in display technologies.<sup>1</sup> In their simplest configuration, a fluorescent semiconducting polymer is sandwiched between two metal electrodes, an anode with a high and a cathode with a low work function. Under the application of an electric field, holes and electrons are injected into the valence and the conduction band of the polymer, respectively. A fraction of these charges combine to form excitons that decay radiatively, giving rise to light emission. While the technology of OLED's is advancing rapidly, fundamental studies of the device operation are lagging behind. Even in PPV derivatives, which were the first polymers to show electroluminescence<sup>2,3</sup> and are by far the best studied, the relative importance of charge injection as opposed to charge transport as the factor limiting the efficiency of OLED's is still under debate.<sup>4-6</sup> For the case of large barriers at the cathode (anode), inefficient electron (hole) injection is the limiting process.<sup>4,7</sup> However, since the trap-free drift mobilities are not known for both carriers, it is not clear whether the efficiency of the best devices is limited by injection or by bulk transport. One experimental degree of freedom is the electrode work function which one can change to alter the barrier for electron or hole injection into the polymer, thus changing the magnitude of the electron (hole) current. Parker<sup>4</sup> has performed a systematic study of (mostly unipolar) devices with different electrode combinations.

In the case of bipolar devices, where there is a significant difference between the work functions of the anode and the cathode, a built-in potential ( $V_{bi}$ ) is established in the polymer layer at zero bias (see Fig. 1).<sup>8</sup> This built-in potential fundamentally affects the operating characteristics of the diode: For applied bias ( $V_{appl}$ ) less than  $V_{bi}$  the electric field inside the polymer opposes charge injection and forward drift current. (Current may flow by diffusion.) In the simplest picture, where the bands of the polymer remain rigid,  $V_{bi}$  is equal to the work-function difference ( $\Delta\phi$ ) between the anode and the cathode. The above picture is surely rather simplistic: Instead of extended bands, the electronic levels of conjugated polymers are best described as a (Gaussian) distribution of localized states. Charge transport takes place by hopping, giving rise to a mobility that is electric-field dependent.<sup>9</sup> Hopping transport in OLED's is discussed in detail elsewhere.<sup>10,11</sup> Moreover, charge accumulation near

the electrodes, pinning of the Fermi level at interface states, formation of a dipole layer or chemical reactions between the metal and the polymer will each result in  $V_{bi} \neq \Delta\phi$ . The critical point remains, however; when the anode and cathode work functions are different, a potential difference is present across the polymer layer. In order to compare data between devices with different anodes or cathodes, this built-in potential must be measured and subtracted from the applied bias. In this way,  $V_{appl} - V_{bi} = 0$  refers to the case of zero average electric field inside the sample (which corresponds to the "flat band" case, if the polymer "bands" remain rigid).

In this paper we discuss the electrical characteristics which dictate the efficiency of MEH-PPV-based light-emitting diodes (where MEH-PPV denotes poly[2-methoxy-5-(2-ethylhexoxy)-1,4-phenylene vinylene]) with Au anodes and Au, Al, and Ca cathodes. By varying the cathode we change the electron current from practically zero (Au) to a maximum value (Ca). For each device, we measure the current and the efficiency as a function of the applied bias. We also measure the built-in potential *on the same device*. We analyze the data in terms of  $V_{appl} - V_{bi}$  and comment on the relative importance of the electron and hole currents. Conclusions on the operation of OLED's are drawn.

The device preparation and characterization procedures can be found in a previous publication.<sup>12</sup> Semitransparent Au anodes were made by vacuum evaporation on glass and were kept immersed in xylene until the casting of the MEH-PPV layer. The built-in potential was determined by both electro-

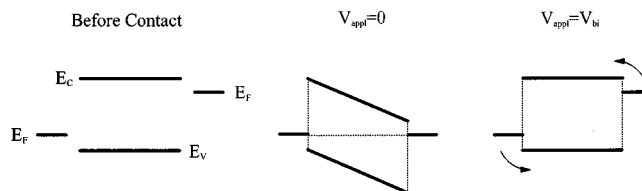


FIG. 1. Schematic illustration of the built-in potential in a fully depleted semiconductor:  $E_F$  depicts the Fermi level of the metal electrode, while  $E_V$  and  $E_C$  the valence and the conduction band of the semiconductor, respectively. Upon contact, a built-in potential, with the opposite sign of forward bias, is established inside the semiconductor, even at zero applied bias. This built-in potential needs to be exceeded before the device will begin operating.

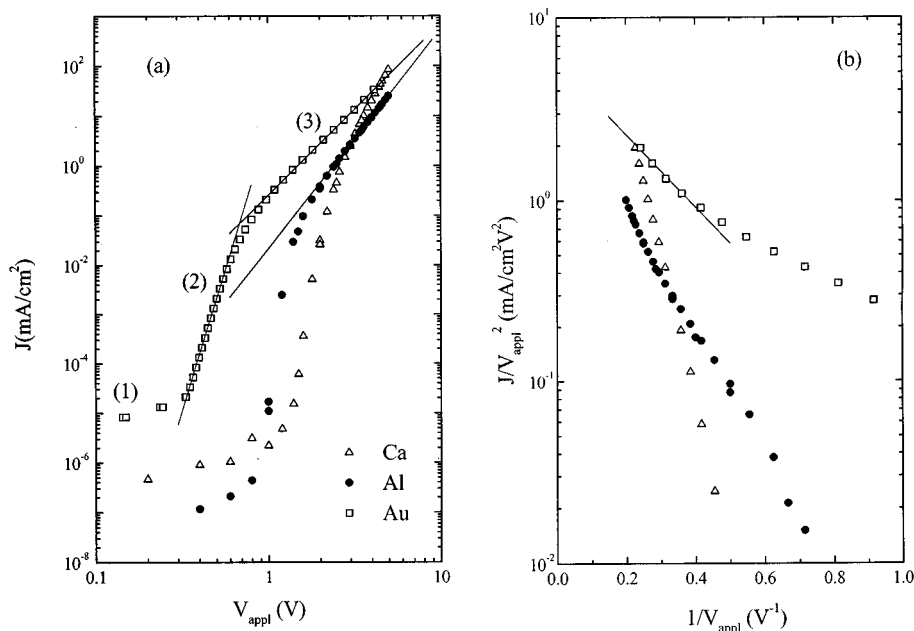


FIG. 2. Current-voltage data from devices with Au (open squares; measured at constant current mode), Al (filled circles), and Ca (open triangles) cathodes. The thicknesses of the MEH-PPV layer were 98 nm (Au cathode), 105 nm (Al), and 101 nm (Ca). (a) Double logarithmic plot. The lines are fits to a power law with slopes equal to 11.4 and 3.4 (Au cathode) and 4.4 (Al cathode). (b) Fowler-Nordheim plot and fit (solid line). See the text for details.

absorption and photovoltaic measurements.<sup>12</sup> A built-in potential was detected even in the sample with two Au contacts, which is rather surprising at first. However, Abkowitz *et al.*<sup>13</sup> have found that Au electrodes evaporated on a small organic molecule layer form injection limited contacts, in contrast with bottom electrodes where the organic is coated on the Au. Luckily, extraction of holes from the top electrode is not affected. We observe a similar behavior in our samples and find that the asymmetry in the current-voltage characteristics is associated with a built-in potential of the order of a few tenths of a volt.

Let us first examine the consequences of using two of the most popular ways described in the literature for analyzing OLED current-voltage data. In Fig. 2(a), the current density is shown as a function of the (uncorrected) applied bias  $V_{\text{appl}}$  on a double logarithmic plot. The curves seem to reveal three different regimes (depicted for the Au/Au curve), which have in the past been attributed to (1) leakage or Ohmic conduction of residual charge inside the sample, (2) injection of charges, and (3) “saturation,” when the current becomes bulk limited.<sup>14</sup> The voltage that corresponds to the transition between regimes (1) and (2) is usually referred to as the “turn-on” voltage, when charge injection begins to take place. The slope of the regime (3) for the Au/Au case is 3.4, which may be analyzed in terms of a trap-limited current (TLC).<sup>15</sup> A power-law dependence of the current with the applied bias has also been observed in OLED’s from PPV (Ref. 5) and from small molecules<sup>16</sup> at voltages above the turn-on. It was attributed to TLC’s and information about the trap density and the effective (and assumed to be constant) mobility was obtained. However, as seen in Fig. 1(a) the slope of the current depends on the cathode. It changes from 3.4 for the Au/Au to 4.4 for the Au/Al sample. Thus, analysis of the data this way implies that electron injection from Al

contributes significantly to the total device current, a conclusion that is inconsistent with the work function of Al, and with the observed quantum efficiency of Au/Al devices.

A second “standard” way of analyzing the current-voltage data is by means of a Fowler-Nordheim (FN) plot,<sup>4</sup> as in Fig. 2(b). Here it is assumed that the current limiting process is the charge injection, which, at high voltages, takes place via FN tunneling. The slope of  $\ln(J/V^2)$  versus  $1/V$  is equal to  $4\sqrt{2m}\phi^{2/3}L/(3\hbar e)$ , where  $m$  is the electron mass,  $\phi$  is the barrier height,  $L$  is the thickness of the sample,  $\hbar$  is Planck’s constant, and  $e$  is the electron charge. Although the data might resemble straight lines at high fields, the barrier height that we obtain for the Au/Au sample is equal to 0.035 eV, comparable to  $kT$  and indicating that the FN formalism is inappropriate for this case. Moreover, the barrier height seems to increase when going to Al and Ca cathodes, which is unphysical.

In both plots of Fig. 2 the data were not corrected for the built-in potential. The shapes of the curves change dramatically when we do so. As seen in Fig. 3(a), the current-voltage relation is no longer a power law over any significant range. Thus, analysis of the data within the framework of TLC’s is no longer intuitive. At the same time, the values for the barrier heights obtained from the FN plot of Fig. 3(b) remain unreasonable. Plotting the data as a function of  $V_{\text{appl}} - V_{\text{bi}}$  not only changes the shape of the curves, but it also reveals some of the physics of device operation. It is now clear that the current for the Au/Al sample is essentially the same as that for the Au/Au sample, as expected from the fact that the barrier for electron injection from Al is of the order of 1 eV.<sup>4,8,12</sup> In contrast, Ca is a very efficient electron injector, causing an increase of almost an order of magnitude in current.

The characteristics of the data in the plotted as in Fig.

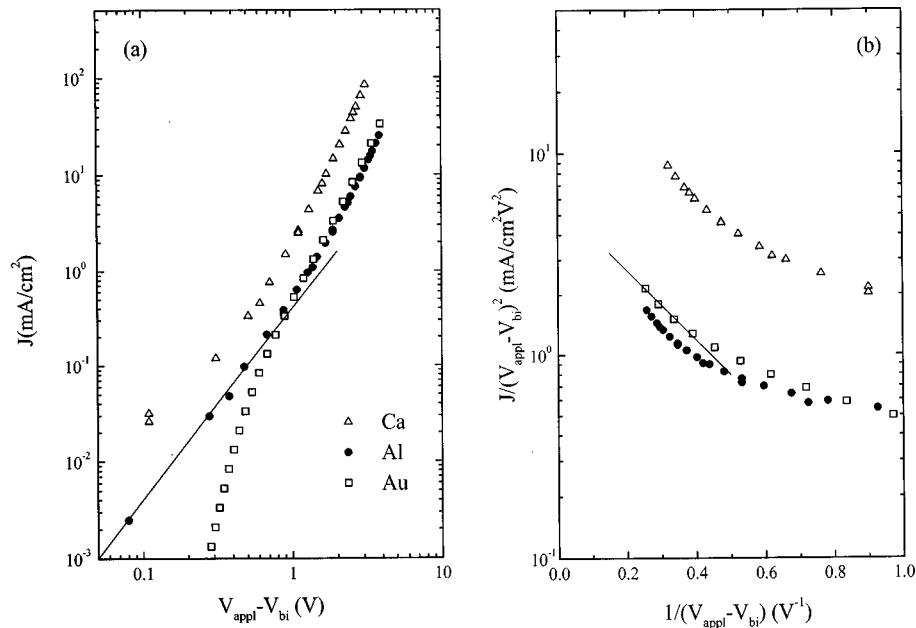


FIG. 3. Current-voltage data from the same devices as in Fig. 2, but corrected for the built-in potential measured on the same devices (0.2 V for Au cathode, 1.1 V for Al, and 1.9 V for Ca, respectively). (a) Double logarithmic plot. The slope of the solid line is equal to 2. (b) Fowler-Nordheim plot and fit (solid line).

3(a), namely a slope near 2 deviating upwards at high voltage, is reminiscent of a space-charge-limited current (SCLC) with a field-dependent mobility. Indeed, Blom *et al.*<sup>6</sup> have determined the hole mobility in a PPV derivative and found that it is electric-field dependent:

$$\mu = \mu_0 \exp(\sqrt{E/E_0}). \quad (1)$$

This dependence, often called ‘‘Poole-Frenkel-like,’’ although the mechanism is now recognized *not* to be Poole-Frenkel,<sup>17</sup> has been explained recently as arising from

energetic disorder due to the interaction of each hopping charge with randomly oriented and randomly located dipoles in the amorphous medium.<sup>18</sup> Murgatroyd<sup>19</sup> was able to show that the current-voltage relation in the case of a mobility as in Eq. (1) could be well approximated by

$$J \approx (9/8) \epsilon \epsilon_0 \mu_0 V^2 \exp(0.89 \sqrt{V/E_0 L}) / L^3, \quad (2)$$

where  $\epsilon \epsilon_0$  is the dielectric constant and  $V = V_{\text{appl}} - V_{\text{bi}}$  in our case. The above equation is derived for monopolar SCLC, but we have been able to show numerically<sup>20</sup> that a similar

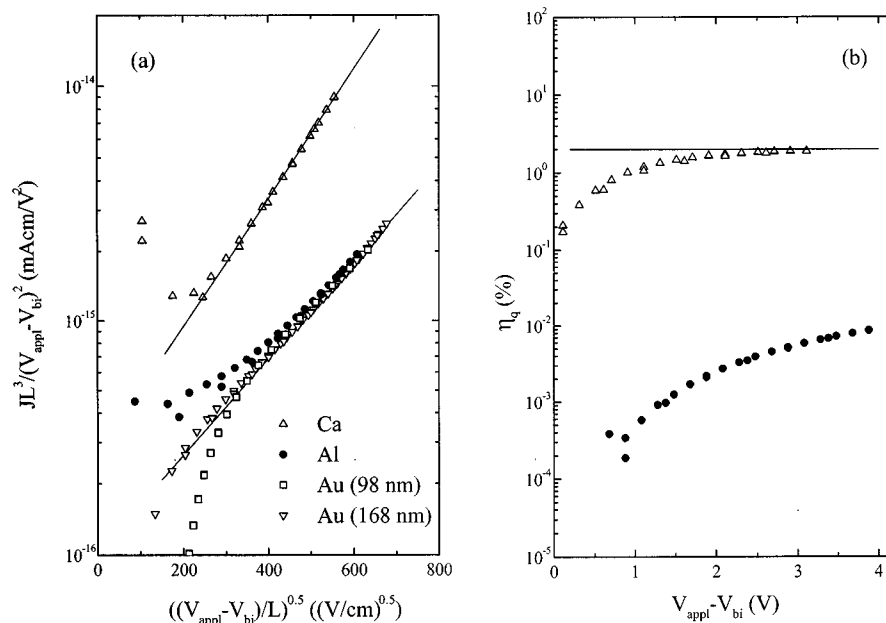


FIG. 4. (a) Current-voltage data from the same devices as in Fig. 3 plotted according to Eq. (2). The open down triangles are from a 168-nm sample with a Au cathode. The lines are fits to Eq. (2). (b) External quantum efficiency for the samples with Al (filled circles) and Ca (open triangles) cathodes. The line indicates the maximum efficiency of 2%.

expression continues to hold for bipolar SCLC although it is not yet clear how the separate field dependencies of the electron and hole mobilities affect the numerical constants.

Following Eq. (2), we replot the data as the logarithm of  $JL^3/V^2$  versus the square root of the mean electric field [Fig. 4(b)]: The slope of a line in this plot gives the characteristic field  $E_0$  and the intercept, the zero-field mobility  $\mu_0$ . The data from the devices with Au and Al cathodes collapse to a single curve at high voltages, as expected. Moreover, Au/Au data from thicker samples (one example is shown with down triangles) show the expected thickness scaling. A fit yields  $\mu_0 = 3.2 \times 10^{-7}$  cm<sup>2</sup>/V sec and  $E_0 = 38$  kV/cm for the hole mobility, in agreement with values for similar PPV derivatives.<sup>6</sup> The sample-to-sample reproducibility of our values is of the order of 25%. The deviation of the data at low voltages is attributed to residual inaccuracy in the determination of the built-in potential, and to differences in the diffusive current for different electrode combinations. The electrical characteristics for the sample with a Ca cathode reveal an *effective* bipolar mobility,<sup>20</sup> with  $\mu_0 = 8.1 \times 10^{-7}$  cm<sup>2</sup>/V sec and  $E_0 = 21$  kV/cm, indicating a strong influence from the electron current.

The external quantum efficiencies of the above devices are shown in Fig. 4(b). We were unable to detect any light from the sample with the Au cathode. Weak emission from the sample with the Al cathode indicates some electron injection, but with electrons carrying less than 1% of the de-

vice current. For the case of a Ca cathode, however, the increased current implies efficient electron injection. The quantum efficiency rises and saturates to 2%, suggesting essentially complete electron-hole recombination and corresponding to a photoluminescence yield of about 35% for MEH-PPV.<sup>21</sup> The fact that maximum efficiency is reached with Au anode and Ca cathode corroborates the conclusion that charge injection in this case poses no limitation and both the electron and the hole currents are space-charge limited.<sup>22</sup> The high bipolar current observed in Au/Ca devices implies that electrons have comparable mobility to holes in MEH-PPV. We have recently verified this by direct measurement of space-charge limited currents in electron-only devices.<sup>23</sup>

In conclusion, we have shown that proper accounting of the built-in potential leads to a consistent analysis of the electrical characteristics of OLED's structures with different electrodes and with difference polymer thicknesses. Au anodes and Ca cathodes can supply space-charge-limited currents to MEH-PPV. By analyzing data from single carrier devices, we have determined the (electric-field-dependent) hole mobility.

This work was supported in part by the Center on Polymer Interfaces and Macromolecular Assemblies (CPIMA), NSF Grant No. DMR-9400354. Thanks are due to Luisa Bozano and Sue Carter (UCSC) for fruitful discussions.

\*Permanent address: Department of Materials Science and Engineering, Cornell University, Ithaca, NY 14853.

<sup>1</sup>*Organic Electroluminescent Materials and Devices*, edited by S. Miyata and H.S. Nalwa (Gordon and Breach, Amsterdam, 1997).

<sup>2</sup>J.H. Burroughes, D.D.C. Bradley, A.R. Brown, R.N. Marks, K. Mackay, R.H. Friend, and A.B. Holmes, *Nature (London)* **347**, 539 (1990).

<sup>3</sup>D. Braun and A.J. Heeger, *Appl. Phys. Lett.* **58**, 1982 (1991).

<sup>4</sup>I.D. Parker, *J. Appl. Phys.* **75**, 1656 (1994).

<sup>5</sup>A.J. Campbell, D.D.C. Bradley, and D.G. Lidzey, *J. Appl. Phys.* **82**, 6326 (1997).

<sup>6</sup>P.W.M. Blom, M.J.M. de Jong, and M.G. van Munster, *Phys. Rev. B* **55**, R656 (1997).

<sup>7</sup>I.H. Campbell, P.S. Davids, D.L. Smith, N.N. Barashkov, and J.P. Ferraris, *Appl. Phys. Lett.* **72**, 1863 (1998).

<sup>8</sup>I.H. Campbell, T.W. Hagler, D.L. Smith, and J.P. Ferraris, *Phys. Rev. Lett.* **76**, 1900 (1996).

<sup>9</sup>P.M. Borsenberger and D.S. Weiss, *Organic Photoreceptors for Electrophotography* (Marcel Dekker, New York, 1993).

<sup>10</sup>E.M. Conwell and M.W. Wu, *Appl. Phys. Lett.* **70**, 1867 (1997).

<sup>11</sup>A. Ioannidis, E. Forthyshe, Y. Gao, M.W. Wu, and E.M. Con-

well, *Appl. Phys. Lett.* **72**, 3038 (1998).

<sup>12</sup>G.G. Malliaras, J.R. Salem, P.J. Brock, and J.C. Scott, *J. Appl. Phys.* **84**, 1583 (1998).

<sup>13</sup>M.A. Abkowitz, J.S. Facci, and J. Rehm, *J. Appl. Phys.* **83**, 2670 (1998); A. Ioannidis, J.S. Facci, and M.A. Abkowitz, *ibid.* **84**, 1439 (1998).

<sup>14</sup>S. Karg, J.C. Scott, J.R. Salem, and M. Angelopoulos, *Synth. Met.* **80**, 111 (1996).

<sup>15</sup>A. Rose, *Concepts in Photoconductivity and Allied Problems* (Interscience, New York, 1963).

<sup>16</sup>P.E. Burrows and S.R. Forrest, *Appl. Phys. Lett.* **64**, 2285 (1994).

<sup>17</sup>J. Frenkel, *Phys. Rev.* **54**, 647 (1938).

<sup>18</sup>D.H. Dunlap, P.E. Parris, and V.M. Kenkre, *Phys. Rev. Lett.* **77**, 542 (1996).

<sup>19</sup>P.N. Murgatroyd, *J. Phys. D* **3**, 151 (1970).

<sup>20</sup>G.G. Malliaras and J.C. Scott (unpublished).

<sup>21</sup>The electroluminescence yield is reduced relative to photoluminescence by a factor of  $\frac{1}{4}$  due to spin statistics, 0.7 due to absorption of the Au anode, and  $\frac{1}{3}$  due to total internal reflection.

<sup>22</sup>G.G. Malliaras and J.C. Scott, *J. Appl. Phys.* **83**, 5399 (1998).

<sup>23</sup>L. Bozano, S.A. Carter, J.C. Scott, G.G. Malliaras, and P.J. Brock (unpublished).